Scaling of the Longitudinal and Hall Resistivities from Vortex Motion in $YBa_2Cu_3O_7$

J. Luo, T. P. Orlando,[a] and J. M. Graybeal[b]
Francis Bitter National Magnet Laboratory, Massachusetts Institute of Technology, Cambridge, Massachusetts 02139

X. D. Wu and R. Muenchausen
Los Alamos National Laboratory, Los Alamos, New Mexico 87545
(Received 30 May 1991; revised manuscript received 4 September 1991)

We measure the longitudinal (ρ_{xx}) and Hall (ρ_{xy}) resistivities as a function of magnetic field and temperature in the mixed state of epitaxial $YBa_2Cu_3O_7$ films. We observe a striking power-law behavior $\rho_{xy}(T) \propto [\rho_{xx}(T)]^{\alpha}$ at fixed field, with $\alpha = 1.7 \pm 0.2$. Our results link the Hall behavior to collective behavior in the presence of pinning. In addition, this power-law dependence is consistent with new calculations for the vortex-glass transition, and therein may provide the first measurement of a new critical exponent.

PACS numbers: 74.60.Ge, 73.50.Jt, 74.40.+k, 74.70.Mq

Following the discovery of high-temperature superconductors (HTSC), intense effort has been directed at understanding the nature of their mixed state. Their considerable anisotropy plus the presence of pinning is expected to significantly enrich the phase diagram in the mixed state [1-3], leading to corresponding questions as to the nature of the vortex dynamics. These are relevant issues, as it is vortex motion that produces dissipation in the mixed state.

Any thorough understanding of the vortex dynamics must encompass both the longitudinal *as well as* the transverse Hall resistivities in the superconducting state. Recent measurements of the vortex Hall behavior in HTSC are strikingly anomalous, both in their dependence as well as their sign [4-9]. Although the relevance of disorder (i.e., pinning) to the longitudinal resistance is well known, this Letter presents the first clear connection between disorder and the Hall behavior. As the study of vortices in the presence of pinning was the original source of the random-field model [10], such studies belong to an important class of disordered systems.

It has recently been proposed that in a penetrating field three-dimensional superconductors will undergo a phase transition into a vortex-glass state, with vanishing resistance at zero frequency [2,3]. Indeed, published measurements for the longitudinal resistance are consistent with this model over the measured range, and provide critical exponents in agreement with theoretical calculations [11]. As the Hall resistance in the mixed state also involves vortex motion, it should thus provide an additional and important experimental test of the putative vortex-glass phase [12].

In what we refer to as conventional flux flow, a finite Hall effect was long ago predicted to arise from the hydrodynamical force on the moving vortices, the so-called Magnus force [13,14]. In the presence of a transport current, vortex motion *perpendicular* to the current is driven by a Lorentz-like force, yielding a finite longitudinal resistivity ρ_{xx}. Additionally, in analogy to translationally invariant fluids, the vortex was predicted to drift with the transport carriers producing a Hall resistivity ρ_{xy} of the same sign as in the normal state. However, no clear confirmation of such Hall behavior has emerged for superconductors, even in conventional systems. Recent measurements strikingly disagree with this behavior, including deviations from the predicted dependences upon field and temperature, as well as sign changes of the Hall effect for $T < T_c$ [4-9]. In fact, similar behavior has been observed in conventional superconductors [15]. As Nernst effect measurements confirm that the observed ρ_{xy} is due to vortex motion [16], the observed behavior of the vortex Hall effect thus clearly poses basic questions for the theory of vortex motion as well as the very nature of the vortex state.

The $YBa_2Cu_3O_7$ (YBCO) films examined were grown on (001) $LaAlO_3$ substrates by pulsed laser deposition [17]. These films are epitaxial ($\hat{c}$ normal to the substrate) and of high quality. Their transition temperatures are $T_c \simeq 90$ K, with high critical current densities of $J_c > 10^6$ A/cm^2 at 77 K. Samples were lithographically patterned using wet etching (1% HNO_3 in H_2O), and evaporated Au layers yielded low-resistance contacts. Two groups of films are used, with thicknesses of $t = 600$ and 1000 Å.

Careful low-noise ac and dc techniques were used to simultaneously measure ρ_{xx} and ρ_{xy} over the range $T \geq 60$ K and $B \leq 23$ T. No dependence of the measured resistivities on the frequency (≤ 1 kHz) and the magnitude ($\leq 5 \times 10^2$ A/cm^2) of the transport current were observed in the region where $\rho_{xy} \neq 0$. The Hall voltage was obtained from the antisymmetric part of the transverse voltage under magnetic field reversal. In our measurements, $\mathbf{B} \perp \mathbf{J}$ and $\mathbf{B} \| \hat{c}$.

Below T_c, ρ_{xy} is a nonlinear function of magnetic field with regions of both positive and negative behavior. Figure 1 compares ρ_{xx} and ρ_{xy} as functions of magnetic field at 86 K for a 600-Å film. The observed onset of finite ρ_{xy} occurs at a higher field than that of ρ_{xx}, although this

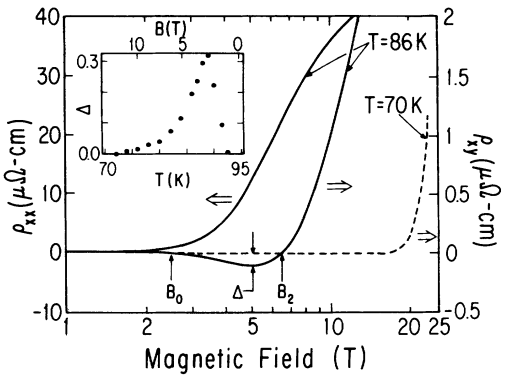

FIG. 1. Longitudinal ρ_{xx} and Hall ρ_{xy} resistivities vs magnetic field at $T=86$ K (600-Å sample). The dashed line shows behavior for ρ_{xy} vs B at $T=70$ K. Inset: The maximum depth Δ of the negative Hall signal vs T (lower scale) and B (upper scale), obtained from ρ_{xy} vs B curves taken at different temperatures.

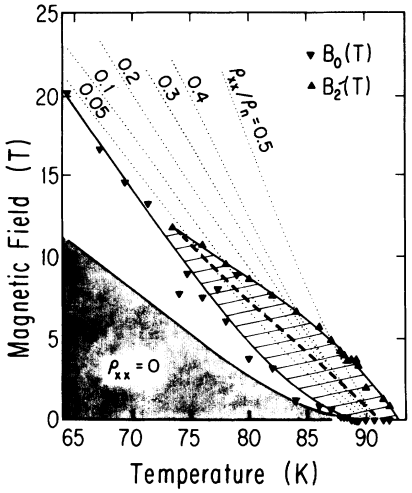

FIG. 2. Vortex behavior in the H-T plane (600-Å sample). Approximate region of $\rho_{xx}=0$ is shaded at lower left. Constant $\rho_{xx}(T)/\rho_n$ curves are dotted lines (ρ_n is the normal-state resistivity). ρ_{xy} is below our measurement threshold to the left of $B_0(T)$, observably negative in the hatched area between $B_0(T)$ and $B_2(T)$, and positive above $B_2(T)$. Dashed line through hatched region indicates loci for the maximum Hall depth.

likely reflects our measurement threshold (10^{-9} V) for the comparatively small Hall voltage. The Hall resistivity is discernibly negative between two characteristic fields B_0 (operationally defined onset for negative ρ_{xy}) and B_2 (operational onset of positive ρ_{xy}). The negative Hall region occurs where ρ_{xx} is increasing rapidly with increasing field. At higher fields ρ_{xy} is positive and increases linearly with field while ρ_{xx} saturates. For $T<75$ K, only positive Hall behavior is observed, as shown by the dashed line in Fig. 1. The inset shows the maximum depth of the negative Hall signal, Δ, as a function of T and B.

Based on families of ρ_{xx} and ρ_{xy} vs B curves we construct the diagram in the H-T plane shown in Fig. 2. The dotted lines denote the position of constant ρ_{xx}/ρ_n, where ρ_n is the normal-state resistivity above T_c. The shaded $\rho_{xx}=0$ region is consistent with the vortex-glass regime [2,11]. Elsewhere, ρ_{xx} is finite. The Hall behavior suggests division into three regions. The region of observed negative ρ_{xy} is the hatched area bordered by the $B_0(T)$ and $B_2(T)$ curves, and extends to high fields for our samples. For $B<B_0$ ρ_{xy} is below our measurement threshold, while for $B>B_2$ ρ_{xy} is positive. The fact that $\rho_{xx}>0$ for all regions where ρ_{xy} is observably nonzero shows that our Hall behavior is associated with the "liquid" phase of mobile vortices. The dashed line through the negative Hall region displays the loci for maximum Hall depth Δ. Although $B_0(T)$ roughly coincides with $\rho_{xx}/\rho_n\approx 0.03$, $B_2(T)$ cuts through the family of ρ_{xx}/ρ_n curves, instead tracking the $\rho_{xx}=0$ boundary. The 1000-Å samples exhibited similar behavior in all regards.

The current-voltage (I-V) characteristics were examined over the (H,T) range covered by Fig. 2. The I-V_{xx} curves were nonlinear in the region between the $\rho_{xx}=0$ and $B_0(T)$ curves, yielding behavior consistent with that obtained by Koch *et al.* [11]. However, for the region of observed nonzero ρ_{xy}, the I-V curves were generally linear for $J\leq 5\times 10^2$ A/cm^2 (above which sample heating occurs). Even at $B_0(T)$ where ρ_{xy} is just zero, we were unable to induce a finite V_{xy} with such current densities. Thus, our Hall data represent the *linear response* of the vortices to the applied current.

Neither ρ_{xx} or ρ_{xy} exhibit simple thermally activated behavior. We find it more insightful to compare the temperature dependences of ρ_{xy} to ρ_{xx}. In Fig. 3 we plot $|\rho_{xy}(T)|$ vs $\rho_{xx}(T)$ on a log-log plot at fixed field. Shown are the data taken at 1.4 and 3.7 T. The cusp is an artifact of the absolute value $|\rho_{xy}|$, corresponding to where $\rho_{xy}(T)$ passes through zero. The data clearly display an

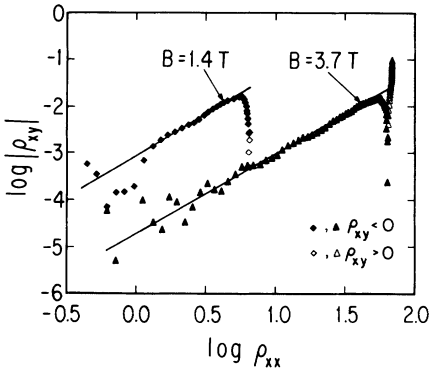

FIG. 3. Log-log plot of $|\rho_{xy}|$ vs ρ_{xx} obtained for temperature sweeps at two magnetic field values (1000-Å sample). Note apparent $|\rho_{xy}|\propto\rho_{xx}^{\alpha}$ behavior with $\alpha=1.7\pm0.2$. Solid symbols for $\rho_{xy}<0$, open for $\rho_{xy}>0$. Units for ρ are $\mu\Omega$ cm.

unexpected and striking power-law relationship in the negative Hall regime. Writing $|\rho_{xy}(T)| \propto [\rho_{xx}(T)]^{\alpha}$, the data yield the value $\alpha = 1.7 \pm 0.2$ for *both* field traces. Thus ρ_{xy} is a stronger function of temperature than ρ_{xx}. At high T, the power-law relationship breaks off abruptly, perhaps signaling the transition to flux flow and/or the normal state. Should the power-law behavior hold to lower temperatures (below our measurement threshold for ρ_{xy}), it would imply that the negative Hall behavior persists all the way to the "vortex-glass" boundary where $\rho_{xx} = 0$ (thereby extending the hatched region of Fig. 2 leftward).

In Fig. 4, we examine the behavior of ρ_{xx} and $|\rho_{xy}(T)|$ within the confines of the vortex-glass model. Choosing a value for T_g consistent with where $\rho_{xx} \to 0$, we obtain $\rho_{xx}(T) \propto (T - T_g)^{\gamma}$ with $\gamma = 6.5$. Such an exponent is consistent with previously obtained theoretical and experimental values [11]. Using the same value of T_g, we again plot our Hall data. $|\rho_{xy}(T)|$ is a steep function of $T - T_g$, varying by three decades in the narrow temperature span of $-1.4 \leq \log[(T - T_g)/T_g] \leq -1.0$. Again, the cusp in $|\rho_{xy}|$ corresponds to where ρ_{xy} passes through zero. Over this narrow span near T_g where ρ_{xy} is observably finite and negative, one thus obtains $|\rho_{xy}(T)| \propto (T - T_g)^{\beta}$ with $\beta = 10.5 \pm 1.5$. Note that for this span of reduced temperature, the corresponding range of ρ_{xx} values are within the critical regime [11]. Although measurement of ρ_{xy} even closer to T_g would reduce the error margin for β, the small size and steep dependence of ρ_{xy} pose clear experimental challenges. However, note from the power-law behavior of Fig. 3, one obtains $\beta = \alpha\gamma = 11.1 \pm 1.2$ for $\gamma = 6.5$.

Reviewing our results, we see that there are three addressable issues regarding the Hall effect in the mixed state: the role of disorder, the observed $|\rho_{xy}(T)| \propto [\rho_{xx}(T)]^{\alpha}$ power-law behavior and its relevance to the nature of the vortex state, and the origin of the negative Hall sign. The degree of interrelationship between these must be considered *carefully*.

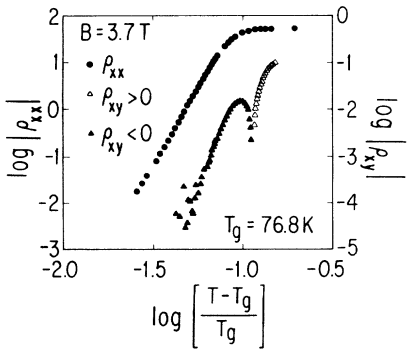

FIG. 4. Log-log plot of $\rho_{xx}(T)$ and $|\rho_{xy}(T)|$ vs $(T - T_g)/T_g$ for $B = 3.7$ T. The *single* fitting parameter used for *both* curves is T_g. Units for ρ are $\mu\Omega$ cm.

It is clear that pinning plays a dominant role in the longitudinal resistance for our samples. The large critical currents and existence of a region with $\rho_{xx} = 0$ attest to this. As vortices are strongly interacting for the field range considered here, we are also observing collective behavior. In view of our power-law relation we thus conclude that the Hall signal also represents collective behavior in the presence of pinning. Furthermore, ρ_{xx} and ρ_{xy} exhibit different sensitivities to the disorder. This difference alone is important.

The nature of the vortex state is itself a controversial issue at the present time. Several theoretical models exist; hence there is a need for additional clear experimental results. In the high-field regime where collective behavior is exhibited, vortex motion is clearly dependent upon the nature of the vortex state. Thus our observed power-law relationship between ρ_{xx} and ρ_{xy}, found in a region where both quantities separately exhibit strong and nontrivial temperature dependences, must be viewed as a key experimental fact to be explained by any candidate model for the vortex phase.

The vortex-glass picture considers the consequences of disorder from the outset. New calculations [12] by Dorsey and Fisher consider the Hall behavior near the glass transition, and are consistent with our data. Note that their scaling analysis *only* addresses the functional dependence but *not* the sign of the Hall effect. They find that the Hall angle should scale to zero at the transition, and there should exist a power-law relation with an exponent $\alpha > 1$. Furthermore, the exponent α can be related to other critical exponents by $\alpha = 1 + \lambda_v/(z + 2 - d)$. Here z is the dynamical exponent, d is the dimensionality, and λ_v is the new particle-hole asymmetry exponent. Within their model, our data provide the first measure of the exponent λ_v, since z has been separately obtained from I-V_{xx} measurements [i.e., the exponent $\gamma = \nu(z + 2 - d)$] [11].

A key strength of their result is that the critical exponent is obtained *independent* of T_g, and *despite* the present inability to explain the Hall sign. Note that for the data in Fig. 3, the vortex-glass correlation lengths inferred from I-V_{xx} curves are consistent with $\xi_z \leq t$ and $\xi_\perp > a_0$. Here t is the film thickness (1000 Å), and a_0 the average vortex spacing. Hence, our data are consistent with being in the 3D limit and within the critical regime. Note that the vortex-glass transition is *not* expected to exist in 2D.

Previous results on 2:2:1:2 Bi-Sr-Ca-Cu-O (BSCCO) crystals ($T_c = 85$ K) by Artemenko, Gorlova, and Latyshev [8] observed *simple* activated behavior in both ρ_{xy} and ρ_{xx} at fixed field. As this differs from our results, we address the key factors. BSCCO crystals are more anisotropic and less disordered than our YBCO films. Both factors significantly reduce the temperature where $\rho_{xx} \to 0$, which may explain the difference in the activation behavior. For YBCO the region where $\rho_{xy} \neq 0$ is very close to T_c and relevant quantities are strongly tempera-

ture dependent; hence simple activated behavior is unlikely. However, the observation that ρ_{xx} and ρ_{xy} had the *same* temperature dependence in BSCCO (i.e., $\alpha \simeq 1$), while our YBCO displays a $\rho_{xy} \propto \rho_{xx}^{1.7}$ behavior is important. Our power-law behavior is nontrivial and *cannot* be explained from a simple model based upon activated behavior. Furthermore, it is such power-law behavior which is characteristic of an incipient second-order transition. The discrepancy in exponents likely originates from the anisotropy difference for the two systems. Indeed, for BSCCO evidence exists that vortices are in the 2D regime for their measured temperature range, so vortex-glass behavior is not expected [18]. Initial results in single 2D thin-film amorphous superconductors additionally point to an exponent $\alpha \simeq 1$ [19]. The fact that BSCCO also has a negative Hall region further emphasizes the separation of the power-law dependence from the Hall sign.

We have withheld the issue of the negative Hall sign until now. The negative sign is *not* universal, and indeed is not observed in our YBCO films at sufficiently high fields. Several models have been introduced to explain the negative Hall sign [6–9]. None can explain our power-law behavior. These models solely modify conventional flux flow while ignoring the consequences of pinning. Recall that in the absence of pinning one is in the conventional flux flow regime where hydrodynamic calculations exist [13,14]. We thus arrive at the following crossroads *vis-à-vis* the negative Hall sign. Either crucial changes in the hydrodynamic model are required, or, should the hydrodynamic model correctly yield a positive Hall sign in the absence of disorder, then disorder must be seen as a crucial element. Motivations exist for either path. The hydrodynamic model ignores the detailed nature of the excitations in the vortex core, which are material specific and include the consequence of band structure [20]. On the other hand, the addition of a random potential strongly modifies vortex motion. In fact, vortex motion between potential minima may not achieve *steady state,* a key assumption of hydrodynamic models. Open questions also exist regarding inhomogeneous flows and/or defect motion in the vortex state, which deserve additional consideration. The origin of the negative Hall sign remains an open question, and awaits additional experiments.

In summary, we have measured both the longitudinal and Hall resistivities in the mixed state for YBCO films. In a region where $\rho_{xx}(T)$ and $\rho_{xy}(T)$ independently exhibit strong and complicated temperature dependences, we observe a striking power-law relationship with $|\rho_{xy}| \propto \rho_{xx}^{\alpha}$ with $\alpha = 1.7 \pm 0.2$. Our results clearly represent the collective vortex response in the presence of disorder. Such power-law dependence is consistent with recent calculations of the vortex-glass model, within which our data would present the first measurement of a new critical exponent λ_v, where $\alpha = 1 + \lambda_v/(z+2-d)$. Our results thus provide new insight into the nature of vortex motion and the nature of the vortex phase.

We gratefully acknowledge the technical assistance of B. Brandt and S. Hannahs at the Francis Bitter National Magnet Laboratory and fruitful discussions with A. Dorsey and M. P. A. Fisher. We acknowledge support from NSF (Grant No. DMR 88-13164), from ONR Contract No. N00014-88-K-0479 (J.M.G.), and from NSF Grant No. DMR 88-02613 (T.P.O.). J.M.G. acknowledges an Alfred P. Sloan Fellowship.

[a]Also at Department of Electrical Engineering and Computer Science, MIT, Cambridge, MA 02139.
[b]Also at Department of Physics, MIT, Cambridge, MA 02139.

[1] D. R. Nelson, Phys. Rev. Lett. **60**, 1973 (1988).
[2] M. P. A. Fisher, Phys. Rev. Lett. **62**, 1514 (1989).
[3] D. S. Fisher, M. P. A. Fisher, and D. A. Huse, Phys. Rev. B **43**, 130 (1991).
[4] M. Galffy and E. Zirngiebl, Solid State Commun. **68**, 929 (1988).
[5] Y. Iye, S. Nakamura, and T. Tamegai, Physica (Amsterdam) **159C**, 616 (1989).
[6] S. J. Hagen, C. J. Lobb, R. L. Greene, M. G. Forrester, and J. H. Kang, Phys. Rev. B **41**, 11630 (1990).
[7] T. R. Chien, N. P. Ong, and Z. Z. Wang (to be published).
[8] S. N. Artemenko, I. G. Gorlova, and Yu. I. Latyshev, Phys. Lett. A **138**, 428 (1989).
[9] S. J. Hagen, C. J. Lobb, R. L. Greene, and M. Eddy, Phys. Rev. B **43**, 6246 (1991).
[10] A. I. Larkin and Yu. N. Ovchinikov, Zh. Eksp. Teor. Fiz. **65**, 1704 (1973); **68**, 1915 (1975) [Sov. Phys. JETP **38**, 854 (1974); **41**, 960 (1975)].
[11] R. H. Koch, V. Foglietti, W. J. Gallagher, G. Koren, A. Gupta, and M. P. A. Fisher, Phys. Rev. Lett. **63**, 1511 (1989).
[12] A. T. Dorsey and M. P. A. Fisher, following Letter, Phys. Rev. Lett. **68**, 694 (1992).
[13] J. Bardeen and M. J. Stephen, Phys. Rev. **140**, A1197 (1965).
[14] P. Nozières and W. F. Vinen, Philos. Mag. **14**, 667 (1966).
[15] K. Noto, S. Shinazawa, and Y. Muto, Solid State Commun. **18**, 1081 (1976).
[16] S. J. Hagen, C. J. Lobb, R. L. Greene, M. G. Forrester, and J. Talvacchio, Phys. Rev. B **42**, 6777 (1990).
[17] X. D. Wu *et al.*, Appl. Phys. Lett. **54**, 1481 (1990).
[18] H. Safar, P. L. Gammel, D. J. Bishop, D. B. Mitzi, and A. Kapitulnik (to be published).
[19] J. Luo, W. White, M. R. Beasley, and J. M. Graybeal (to be published).
[20] Salman Ullah and Alan T. Dorsey, Phys. Rev. B **44**, 262 (1991).

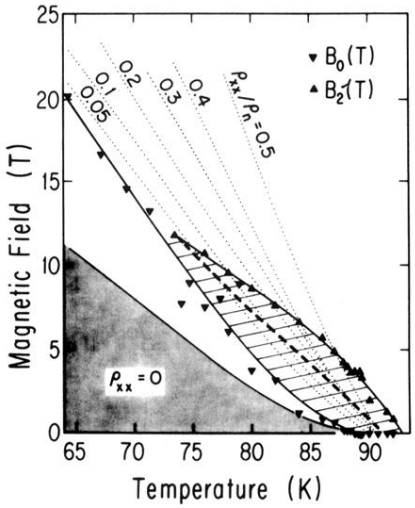

FIG. 2. Vortex behavior in the H-T plane (600-Å sample). Approximate region of $\rho_{xx}=0$ is shaded at lower left. Constant $\rho_{xx}(T)/\rho_n$ curves are dotted lines (ρ_n is the normal-state resistivity). ρ_{xy} is below our measurement threshold to the left of $B_0(T)$, observably negative in the hatched area between $B_0(T)$ and $B_2(T)$, and positive above $B_2(T)$. Dashed line through hatched region indicates loci for the maximum Hall depth.